Synthesis and crystal structures of two lead(II) complexes of 4,4,4-trifluoro-1-naphthyl-1,3-butanedione ligand, subtle interplay of weak intermolecular interactions

Farzin Marandi[a]; Zohreh Hanasavi[b]; Hossein Farzaneh[c]

[a] Department of Science, Payame Noor University (PNU), Zanjan, Iran [b] Department of Science, Payame Noor University (PNU), Abhar, Iran [c] Department of Chemistry, University of Zanjan, Zanjan, Iran

PLEASE SCROLL DOWN FOR ARTICLE

Taylor & Francis
Taylor & Francis Group

Synthesis and crystal structures of two lead(II) complexes of 4,4,4-trifluoro-1-naphthyl-1,3-butanedione ligand, subtle interplay of weak intermolecular interactions

FARZIN MARANDI*†, ZOHREH HANASAVI‡ and HOSSEIN FARZANEH§

†Department of Science, Payame Noor University (PNU), Zanjan, Iran
‡Department of Science, Payame Noor University (PNU), Abhar, Iran
§Department of Chemistry, University of Zanjan, Zanjan, Iran

$[Pb_2(tfnb)_4(\mu\text{-}CH_3OH)]_n$ (1) and $[Pb_2(dmp)_2(tfnb)_4]$ (2) (tfnb and dmp are the abbreviations for 4,4,4-trifluoro-1-naphthyl-1,3-butanedionate and 2,9-dimethyl-1,10-phenanthroline) have been synthesized and characterized by elemental analysis, IR, ^1H NMR spectroscopy, and thermal analysis. The single-crystal structure of 1 shows that the complex forms two 1-D polymeric networks containing four types of Pb^{2+} with coordination numbers seven for Pb(1) and Pb(3), five for Pb(2), and six for Pb(4). The single-crystal structure of 2 shows that the complex forms a dinuclear complex with eight-coordinate Pb(II). The supramolecular features in this complex are guided by lone-pair activity and the control of weak directional intermolecular interactions and aromatic π–π stacking interactions.

1. Introduction

Metal-organic coordination polymers are an emerging area of interest with a variety of supramolecular architectures used in magnetism [1, 2], optoelectronics [3], guest exchangeability [4, 5], and catalysis [6]. Crystal engineering was first introduced as an approach to more efficient topochemical reactions in the early 1960s [7]. However, the synthesis of coordination polymers using crystal engineering was not achieved until 1995 [8, 9]. Several recent reviews have described how coordination polymers ranging from 1-D to 3-D arise from crystal engineering [10, 11]. Crystal engineering via hydrogen bonding has attracted interest ([12] and references therein) and weak C–H$\cdots\pi$, π–stacking and C–H$\cdots$O interactions have also been used [13]. Organohalogen compounds generate motifs via C–H$\cdots$X, X$\cdots$X, and C–X$\cdots\pi$ interactions [14], but fluorine does not readily accept hydrogen bonds and behaves differently from chlorine and bromine [15]. Chopra and Row ([16] and references therein) have shown that a significant number of compounds pack via weak interactions involving organic fluorine packing motifs via F$\cdots$F, C–H$\cdots$F, and C–F$\cdots\pi$ interactions. Research is being

---

*Corresponding author. Email: fmarandi2004@yahoo.com

carried out in the field of bioactive compounds of pharmaceutical and agrochemical interest [17] and to evaluate the importance of organic fluorine in such compounds [16, 18]. In an effort to explore weak interactions, lead(II) complexes with β-diketonates and neutral diimine chelating ligands have been synthesized and determined by X-ray crystal structure [19–22]. In this article we report the synthesis and crystal structures of $[Pb_2(tfnb)_4(\mu\text{-}CH_3OH)]_n$ (1) and $[Pb_2(dmp)_2(tfnb)_4]$ (2).

2. Experimental

2.1. *Physical measurements*

All reagents were purchased from Acros and Merck and used without purification. All solvents were of analytical grade and used without purification. IR spectra were recorded as nujol mulls using Perkin–Elmer 597 and Nicolet 510P spectrophotometers. Microanalyses were carried out using a Heraeus CHN–O-Rapid analyzer. The Pb analysis was carried out by Atomic Absorption (VARIAN SS240 instrument). Melting points were measured on an Electrothermal 9100 apparatus and are uncorrected. ^{1}H NMR spectra were measured with a BRUKER DRX-500 AVANCE spectrometer at 500 MHz. Thermal analyses were carried out on a Perkin–Elmer instrument (Seiko Instruments).

2.2. *Preparation of $[Pb_2(tfnb)_4(\mu\text{-}CH_3OH)]_n$ (1)*

4,4,4-Trifluoro-1-naphthyl-1,3-butanedionate, Htfnb, (0.266 g, 1 mmol) was placed in one arm of a branched tube ([23] and references therein) and lead(II) acetate (0.379 g, 1 mmol) in the other. Methanol was carefully added to fill both arms, the tube was sealed, and the ligand-containing arm was immersed in a bath at 60°C while the other was at ambient temperature. After 5 days, crystals deposited in the cooler arm were filtered off, washed with ether, and dried, yield: 70%, Analysis: Found (%): C: 45.65, H: 2.70, Pb: 27.40. Calculated for $C_{57}H_{36}F_{12}O_9Pb_2$ (%): C: 45.38, H: 2.38, Pb: 27.46. IR (cm^{-1}) bands: 701(m), 1018(m), 1149(s), 1280(s), 1410(s), 1473(s), 1573(s), 2990(w), and 3070(w). ^{1}H NMR (DMSO, δ): 3.15(q, 1H), 3.30(m, 3H), 6.20(s, 4H), 7.51(m, 8H), 7.88(m, 16H), 8.40(m, 4H).

2.3. *Preparation of $[Pb_2(dmp)_2(tfnb)_4]$ (2)*

4,4,4-Trifluoro-1-naphthyl-1,3-butanedionate, Htfnb, (0.266 g, 1 mmol) and 2,9-dimethyl-1,10-phenanthroline (0.104 g, 0.5 mmol) were placed in one arm of a branched tube and lead(II) acetate (0.190 g, 0.5 mmol) in the other. Methanol was carefully added to fill both arms, the tube was sealed, and the ligand-containing arm was immersed in a bath at 60°C while the other was at ambient temperature. After 4 days, crystals deposited in the cooler arm were filtered off and dried, yield: 65%, m.p. 165°C. Analysis: Found (%): C: 53.66, H: 2.64, N: 3.25. Calculated for $C_{42}H_{28}F_6N_2O_4Pb$ (%): C: 53.27, H: 2.95, N: 2.95.

IR (cm^{-1}) bands: 701(m), 1018(m), 1149(s), 1280(s), 1410(s), 1473(s), 1573(s), 2990(w) and 3070(w). ^{1}H NMR (DMSO, δ): 2.85(s, 6H), 6.20(s, 2H), 7.51(m, 4H), 7.60(d, 2H), 7.88(m, 8H), 7.95(s, 2H), 8.40(m, 2H), 9.25(d, 2H).

2.4. *Crystallography*

Data were collected with a Nonius KappaCCD, Mo-Kα radiation ($\lambda = 0.71073$ Å) and graded multilayer X-ray optics. Structure solution was performed with SIR97 by direct methods [24] and refined by full-matrix least-squares on F^2 with SHELXL-97 [25]. All non-hydrogen positions were found and refined with anisotropic temperature factors. Materials for publication were prepared using SHELXTL [26] and ORTEPIII [27].

3. Results and discussion

3.1. *Spectroscopic studies*

IR spectra display characteristic absorption bands for ''dmp'' and ''tfnb'' anions. The relatively weak absorption bands at 3065 and 3075 cm^{-1} are due to the C–H modes involving aromatic hydrogens. The C–H modes of aliphatic hydrogens of ''dmp'' were at 2990 cm^{-1}. Absorption bands with variable intensity in the frequency range 1400–1580 cm^{-1} correspond to aromatic ring vibrations of ''dmp'' and ''tfnb''. Absorption bands with variable intensity from 1100 to 1350 cm^{-1} correspond to C–F vibrations of ''tfnb''. The ^{1}H NMR spectrum (DMSO) of **2** at 7.50–9.50 ppm displays three different protons of py groups of ''dmp''. Three distinct peaks at 7.5–8.5 ppm were assigned to protons of naphthyl. The proton of methine, =CH–, is a singlet at 6 ppm for both complexes. The ^{1}H NMR spectrum of **2** shows another band at 2.85 ppm assigned to the methyl of ''dmp''.

3.2. *Description of crystal structures*

Compound **1** crystallizes in the monoclinic space group *P21/c* (table 1). The asymmetric unit of **1** contains two [(tfnb)$_2$Pb(μ-CH$_3$OH)Pb(tfnb)$_2$]. The ORTEP is shown in figure 1 and selected bond lengths and angles are given in table 1. The solid-state structure of **1** reveals that both moieties act as monomers of two 1-D coordination polymers along [001] established by μ-O–Pb contacts (Pb1–O6–Pb2, Pb1–O17–Pb2^i, Pb3–O14–Pb4, and Pb3–O18–Pb4^i). These polymeric strands are stabilized by hydrogen bonds (O4$\cdots$O17 with a distance of 2.782 Å and O12$\cdots$O18 with a distance of 2.825 Å) and weak Pb–O bonds (Pb2–O3 with a distance of 3.080 Å (dashed bond in figure 1) and Pb4–O11 with a distance of 3.042 Å). The coordination numbers of the four symmetrically independent Pb^{2+} are seven for Pb(1), Pb(2), Pb(3) and six for Pb(4) (figure 2). The tfnb is both a bidentate and a bridging group (tridentate) in both polymeric strands. The arrangement of these ligands suggests a gap in the coordination geometry around the metal ions (for Pb1, O6–Pb1–O17 angle is 141.31(8)°, for Pb2 and Pb4 the presence of gap is clear (angles are >180°) and for Pb3, O14–Pb3–O18 angle is 147.09(8)°) occupied possibly by a stereo-active lone pair of electrons on lead(II) [28].

Table 1. Crystal data and structure refinement for **1** and **2**.

Identification code	**1**	**2**
Empirical formula	$C_{57}H_{36}F_{12}O_9Pb_2$	$C_{84}H_{56}F_{12}N_4O_8Pb_2$
Formula weight	1507.30	1891.73
Temperature (K)	200	100.0(2)
Wavelength (Å)	0.71073	0.71073
Crystal system	Monoclinic	Triclinic
Space group	*P*2$_1$/*c*	*P*$\bar{1}$
Unit cell dimensions (Å, °)		
a	23.3611(2)	11.1267(14)
b	26.7539(2)	12.3493(15)
c	16.3412(1)	14.856(4)
α	90.00	96.719(14)
β	90.5224(6)	106.093(15)
γ	90.00	111.450(11)
Volume (Å^3), *Z*	10212.83(13), 8	1770.2(6), 1
Calculated density (g cm^{-3})	1.961	1.7746(6)
Absorption coefficient (mm^{-1})	6.689	4.844
F(000)	5776	924
Crystal size (mm^3)	$0.2 \times 0.12 \times 0.09$	$0.18 \times 0.06 \times 0.03$
θ range for data collection (°)	3.1–27.5	3.7–25.0
Limiting indice	$-30 \leq h \leq 30$; $-32 \leq k \leq 34$; $-21 \leq l \leq 21$	$-12 \leq h \leq 13$; $-14 \leq k \leq 12$; $-17 \leq l \leq 14$
Reflections collected	145,019	12,085
Independent reflections	23397 [*R*(int) = 0.052]	6097 [*R*(int) = 0.040]
Refinement method	Full-matrix least-squares on F^2	Full-matrix least-squares on F^2
Data/restraints/parameters	23,397/0/1451	6097/0/492
Goodness-of-fit on F^2	1.037	0.98
Final *R* [$I > 2\sigma(I)$]	$R_1 = 0.0326$, $wR_2 = 0.0624$	$R_1 = 0.0328$; $wR_2 = 0.0625$
R indices (all data)	$R_1 = 0.0577$; $wR_2 = 0.0675$	$R_1 = 0.0476$; $wR_2 = 0.0672$
Largest difference peak and hole (e Å^{-3})	0.952 and -1.315	2.014 and -1.283

The observed shortening of the Pb–N bonds on the side of Pb(II) opposite to the putative lone pair (in Pb1, 2.355(3) Å compared with 2.925(2) Å adjacent to the lone pair, in Pb2, 2.344(2) Å compared with 2.788(3) Å adjacent to the lone pair, in Pb3, 2.315(3) Å compared with 3.024(3) Å adjacent to the lone pair and in Pb4, 2.315(3) Å compared with 3.042(3) Å adjacent to the lone pair) supports its presence [29]. Hence, the coordination environment of every lead is likely caused by the geometrical constraints of coordinated tfnb ligands and by the influence of a stereo-chemically active lone pair of electrons on the metal. Such an environment leaves space for the interaction of fluorine and oxygen of tfnb of adjacent molecules. The Pb1 and Pb3 atoms interact with fluorine of tfnb with distances of 3.622(3) and 3.840(4) Å, respectively, and Pb2 and Pb4 interact with fluorine and oxygen of tfnb with distances of 3.579(3), 3.728(4), 3.957(4) Å and 3.387(4), 3.728(4), 3.392(4), 3.811(4) Å, respectively (table 2 and figure 2) [30].

Compound **2** crystallizes in the triclinic space group *P*$\bar{1}$ (table 1). Selected bond distances and angles are listed in table 2. Each asymmetric unit contains a Pb(II), two "tfnb" anions and a dmp. The complex can be considered as dimers of lead(II) coordinated by the two "dmp" ligands and four "tfnb$^-$" anions (figure 3). The coordination number of lead is eight (two of "dmp" and six of "tfnb"). Each Pb along with six normal bonds forms two weak Pb$\cdots$O bonds yielding the two Pb_2O_2
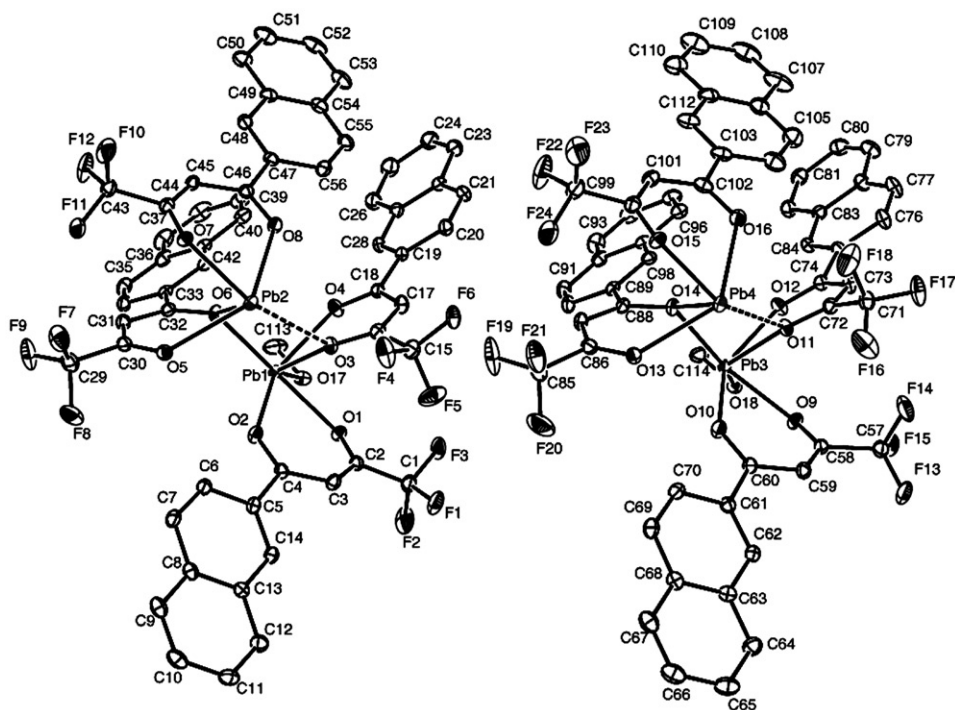
Figure 1. ORTEP presentation of the two [Pb$_2$(tfnb)$_4$(μ-CH$_3$OH)] moieties of **1** in the asymmetric unit. Hydrogen atoms omitted and some carbon atoms not labeled for clarity.

rhombuses [30], with distances Pb1–O3 = 2.692(4) Å, Pb1–O4 = 2.891 Å, Pb1–O3^i = 3.016(4) Å, Pb1–O4^i = 2.819(4) Å. The presence of a lone pair on lead is apparently the reason that the bridging interactions are so long. A useful comparison of **2** is provided by a recent structural study of the dinuclear complexes of Pb^{II} with fluorinated β-diketonate. The Pb–N bond lengths of 2.667(5) and 2.676(4) Å are within the range of similar Pb–N aromatic (dmp ligand) bonding distances (from 2.582(2) and 2.768(1) Å) and the Pb–N bond length with dmp is longer than phen in complexes of β-diketonates [22] and related structures of lead(II) complexes with 1,10-phenanthroline [31]. The C–O bond length of diketonate in **2** is within the range of similar C–O bonding distance from 1.23 to 1.27 Å [22].

A search was made for weak directional intermolecular interactions in the structures of **1** and **2**. An interesting feature in **1** and **2** are the C–F · · · H–C interactions with the distances ranging from 2.339 to 2.525 Å and C–H · · · O from 2.369 to 2.470 Å [16], suggesting strong interactions within this class of weak non-covalent contacts [32, 33] (table 3). There are short F · · · F interactions in **1**, with distances 2.767(4), 2.778(4), 2.780(4), 2.863(4), 2.885(5), and 2.898 Å, less than the sum of the van der Waals radii for fluorine at 2.94 Å (figure 4) [34]. The packing diagrams of these complexes exhibit structural topologies via three different π–π stacking in **1** (edge-to-edge with distances of 3.459, 3.463, and 3.471 Å, face-to-face with distance of 3.408 Å and slipped face-to-face with distance of 3.482 Å) and two different π–π stacking in **2** (figure 5) (face-to-face with distance of 3.427 Å and slipped face-to-face with distance of 3.468 Å), appreciably
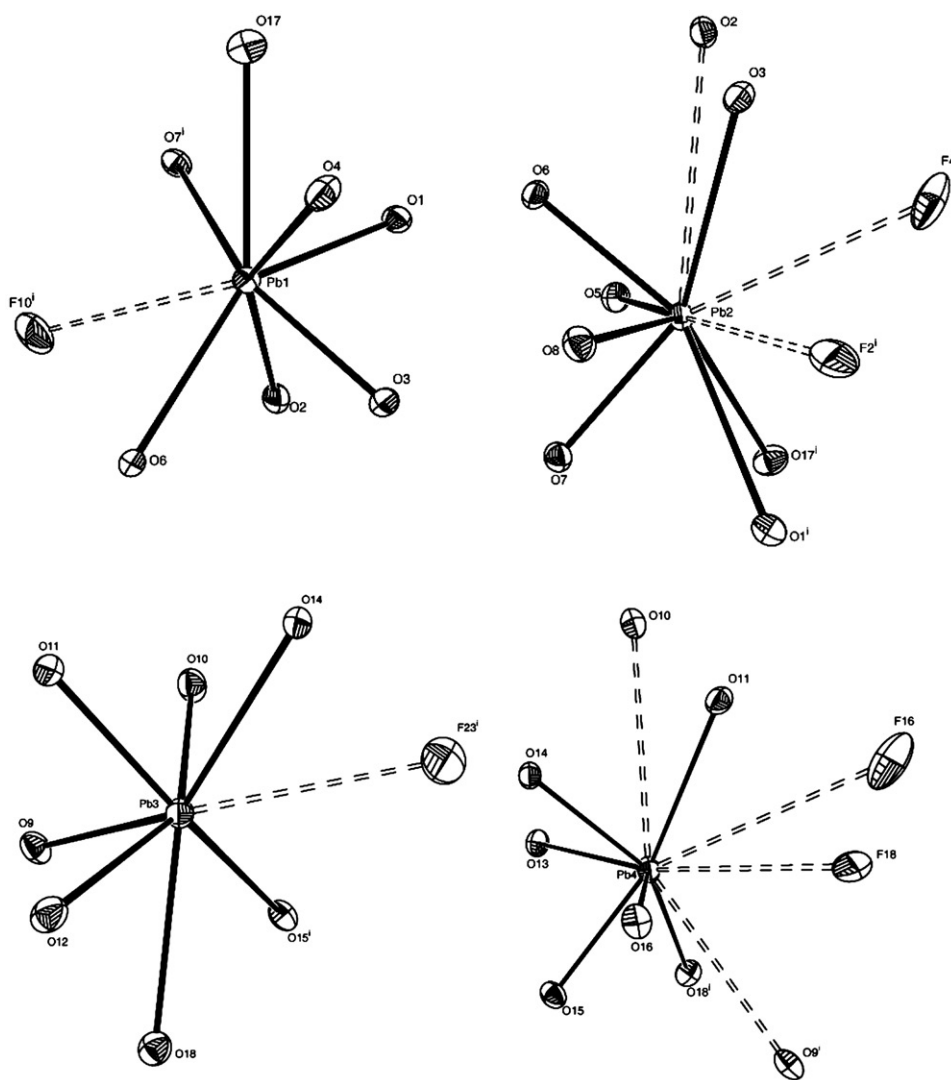
Figure 2. Schematic representation of the four different types of Pb^{II} environments in **1**.

shorter than normal π–π stacking [35, 36]. Consequently, the π–π stacking and F$\cdots$HC, O$\cdots$HC, and F$\cdots$F interactions allow the two 1-D coordination polymers and dinuclear complexes to form a hybrid three-dimensional network.

3.3. Thermal studies

To study the stability of the compounds, thermogravimetric analyses (TGA) for these complexes were performed on polycrystalline samples under nitrogen. Compound **1** does not melt and is stable to 280°C. "tfnb$^-$" decompose in a two-step mechanism in the temperature range 280–320°C and 480–550°C with exothermic effects. The solid

Table 2. Selected bond lengths (Å) and angles (°) for **1** and **2**.

1

|	Pb1			Pb3	
Pb1–O1		2.355(3)	Pb3–O9		2.315(3)
Pb1–O3		2.375(3)	Pb3–O11		2.376(3)
Pb1–O2		2.408(3)	Pb3–O10		2.394(3)
Pb1–O4		2.508(3)	Pb3–O12		2.477(3)
Pb1–O6		2.738(2)	Pb3–O14		2.820(3)
Pb1–O17		2.846(3)	Pb3–O18		2.861(3)
Pb–O7^i		2.925(2)	Pb3–O15^i		3.024(3)
Pb1$\cdots$F10^i		3.622(3)	Pb3$\cdots$F23^i		3.861(3)
O1–Pb1–O3		80.54(9)	O14–Pb3–O18		147.09(8)
O3–Pb1–O2		77.36(9)	O10–Pb3–O12		146.96(9)
O1–Pb1–O4		88.53(9)	O10–Pb3–O18		128.64(9)
O2–Pb1–O4		147.15(8)	O10–Pb3–O15^i		73.60(9)
O1–Pb1–O6		146.72(8)	O12–Pb3–O14		107.85(9)
O3–Pb1–O6		73.30(8)	O11–Pb3–O18		130.35(9)
O2–Pb1–O6		78.78(8)	O9–Pb3–O12		81.62(9)
O4–Pb1–O6		102.04(9)	O9–Pb3–O14		141.16(8)
	Pb2			Pb4	
Pb2–O7		2.316(2)	Pb4–O15		2.315(3)
Pb2–O6		2.344(2)	Pb4–O14		2.337(3)
Pb2–O8		2.409(3)	Pb4–O16		2.409(3)
Pb2–O5		2.478(3)	Pb4–O13		2.457(3)
Pb2–O17^i		2.788(3)	Pb4–O18^i		2.846(3)
Pb2–O1^i		3.056(4)	Pb4–O11		3.042(3)
Pb2–O3		3.080(4)	Pb4$\cdots$O9		3.392(4)
Pb2$\cdots$F2^i		3.728(4)	Pb4$\cdots$O10		3.811(4)
Pb2$\cdots$F4		3.579(3)	Pb4$\cdots$F18		3.387(4)
O5–Pb2–O7		73.61(9)	Pb4$\cdots$F16		3.728(3)
O5–Pb2–O8		131.21(9)	O11–Pb4–O15		142.22(8)
O6–Pb2–O17^i		140.44(9)	O11–Pb4–O13		118.95(8)
O6–Pb2–O7		89.63(8)	O13–Pb4–O16		131.95(9)
O6–Pb2–O8		73.62(9)	O14–Pb4–O18^i		142.86(9)
O8–Pb2–O17^i		128.81(9)	O14–Pb4–O15		91.45(9)
O7–Pb2–O1^i		70.87(9)			

$^i x, -y + 1/2, z + 1/2.$

2

Pb–O1	2.455(4)	Pb–N1	2.667(5)
Pb–O2	2.489(4)	Pb–N2	2.676(4)
Pb–O3	2.692(4)	Pb–O3^i	3.016(4)
Pb–O4	2.861(4)	Pb–O4^i	2.819(4)
O1–Pb–O3	78.27(12)	O2–Pb–N1	85.02(13)
O1–Pb–O4	120.29(12)	O2–Pb–N2	117.61(12)
O1–Pb–N1	114.11(13)	O2–Pb–O3^i	120.90(12)
O1–Pb–O3^i	168.82(13)	O3^i–Pb–N1	70.94(13)
O1–Pb–O4^i	110.09(12)	O3–Pb–N1	166.40(14)
O2–Pb–O3	94.57(13)	O3–Pb–N2	128.13(14)
O3^i–Pb–O4	65.54(11)	O4–Pb–O4^i	97.25(11)
O4^i–Pb–N1	108.25(12)	O3^i–Pb–N2	98.25(12)

$^i -x, -y, -z.$

residue formed is PbO (observed 29.1%, Calcd 29.6%). The TG curve of **2** indicates that it melts at 165°C and begins to decompose at 200°C. The "dmp" and "tfnb⁻" decompose at 200–260°C and 400–550°C with exothermic effects. The solid residue formed is PbO (observed 24.1%, Calcd 24.6%) (figure S6). Atomic absorption supported the presences of PbO residue. These compounds are potential source precursors for lead oxides materials.
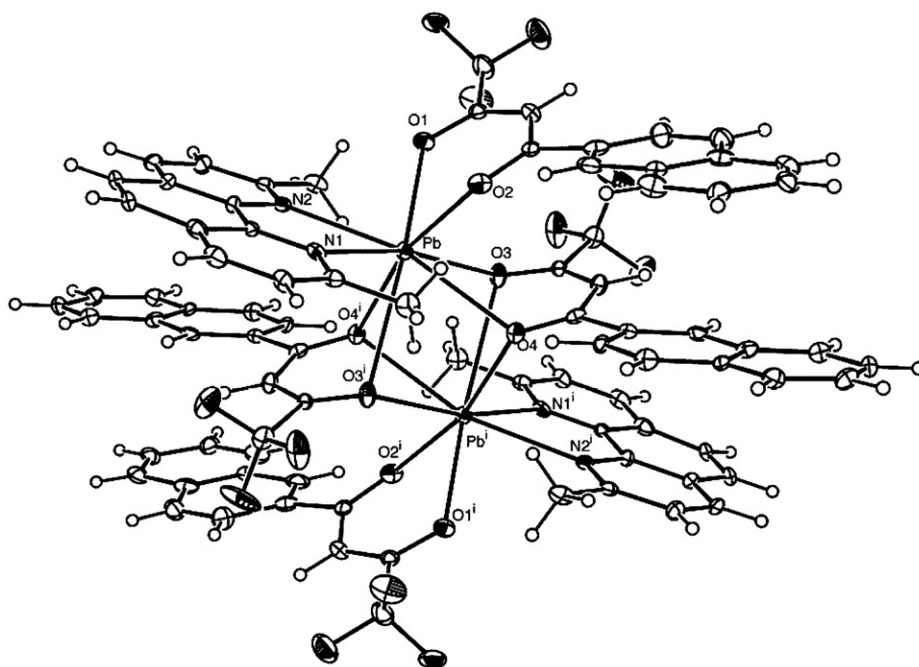
Figure 3.   ORTEP presentation (40% ellipsoid probability) of **2** in the asymmetric unit.

Table 3.   Intermolecular interactions in crystals of **1** and **2**.

B–H···A	H···A (Å)	B···A (Å)	B–H···A (°)
1			
C3– H3···F1	2.339	2.728(5)	103.94
C113–H11c^i···F7	2.513	3.417(6)	153.38
C28–H28···O4	2.391	2.728(5)	100.43
C31–H31···F9	2.348	2.721(5)	102.80
C45–H45···F12	2.354	2.728(4)	102.84
C59–H59···F13	2.414	2.769(4)	101.74
C73–H73···F17	2.362	2.749(5)	103.83
C84–H84···O12	2.374	2.716(5)	100.75
C87–H87···F6	2.525	3.463(4)	168.73
C87–H87···F19	2.349	2.719(5)	102.51
C101–H101···F22	2.399	2.750(5)	101.50
C104–H104···O16	2.369	2.708(6)	100.54
C17–H171···F6	2.392	2.759(5)	102.55
$^i x, y + 1/2, z + 1/2$.			
2			
C3–H3···F1	2.34	2.733(8)	104.00
C33–H33···O1^i	2.44	3.293(8)	149.00
C34–H34···O2^i	2.59	3.295(7)	131.00
C41–H41A···O3^i	2.59	3.295(7)	139.00
C41–H41C···O2	2.42	3.319(7)	152.00
C42–H42A···O1	2.42	3.021(7)	119.00
C42–H42C···O4^i	2.47	3.354(7)	149.00
$^i 1-x, 2-y, -z$.			
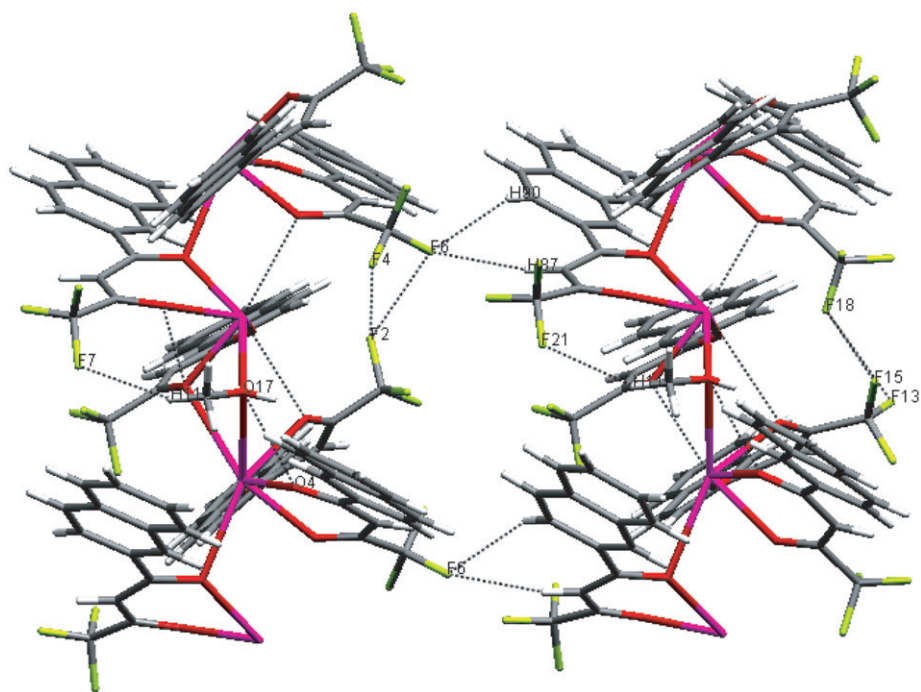
Figure 4.   A view down *b*, packing of **1** chains to form 3-D supramolecular layers via "O $\cdots$ HC, F $\cdots$ HC, F $\cdots$ F, and π–π interactions" (all interactions are in table 3).
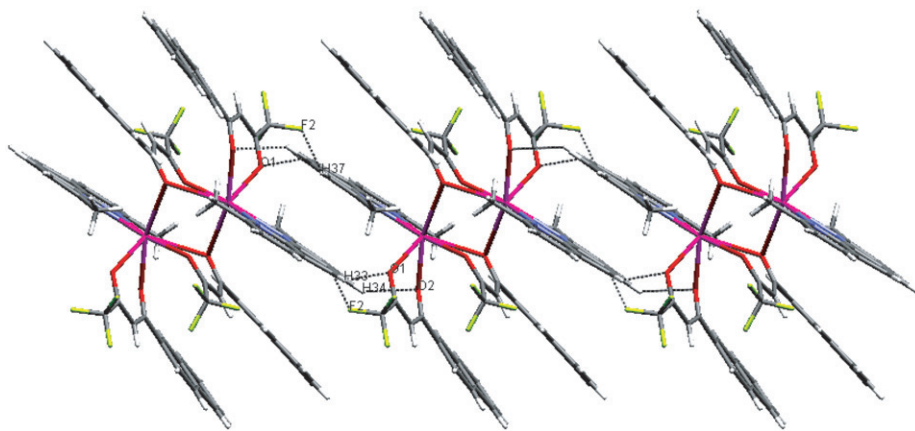
Figure 5.   A view down *a*, packing of **2** to form 2-D supramolecular layers via "O $\cdots$ HC, F $\cdots$ HC, and π–π interactions" (all interactions are in table 3).

4. Conclusion

A subtle interplay among lone pair activity, strong and weak interactions appears to control packing motifs in the crystal structure of **1** and **2**. Our results suggest that, while interactions involving "organic fluorine" have a significant influence in generating

supramolecular assemblies in inorganic solids, the general use of these interactions for *a priori* prediction of packing motifs is yet to be harnessed.

Supplementary material

Crystallographic data for the structure reported in this article have been deposited with the Cambridge Crystallographic Data Centre as supplementary publication No. CCDC-650412 and 720075 for **1** and **2**. Copies of the data can be obtained on application to CCDC, 12 Union Road, Cambridge CB2 1EZ, UK [Fax: +44–1223/ 336033; Email: deposit@ccdc.cam.ac.uk].

Acknowledgment

References

[1] X.Y. Wang, B.L. Li, X. Zhu, S. Gao. *Eur. J. Inorg. Chem.*, **16**, 3277 (2005).
[2] K. Inoue, T. Hayamizu, H. Iwamura, D. Hashizume, Y. Ohashi. *J. Am. Chem. Soc.*, **118**, 1803 (1996).
[3] O.R. Evans, W.B. Lin. *Chem. Mater.*, **13**, 2705 (2001).
[4] O.M. Yaghi, C.E. Davis, G.M. Li, H.L. Li. *J. Am. Chem. Soc.*, **119**, 2861 (1997).
[5] S. Kawata, S. Kitagawa, H. Kumagai, C. Kudo, H. Kamesaki, T. Ishiyama, R. Suzuki, M. Kondo, M. Katada. *Inorg. Chem.*, **35**, 4449 (1996).
[6] K. Endo, T. Kake, T. Sawaki, O. Hayashida, H. Masuda, H. Aoyama. *J. Am. Chem. Soc.*, **119**, 4117 (1997).
[7] B.F. Hoskins, R. Robson. *J. Am. Chem. Soc.*, **112**, 1546 (1990).
[8] S. Mann. *J. Chem. Soc., Dalton Trans.*, 1 (1993).
[9] L.R. MacGillivray, S. Subramanian, M.J. Zaworotko. *Chem. Commun.*, 1325 (1994).
[10] K. Biradha, M. Sarkar, L. Rajput. *Chem. Commun.*, 4169 (2006).
[11] N.W. Ockwig, O. Delgado-Friedrichs, M. O'Keeffe, O.M. Yaghi. *Acc. Chem. Res.*, **38**, 176 (2005).
[12] G.R. Desiraju. *Acc. Chem. Res.*, **35**, 565 (2002).
[13] T. Steiner. *Angew. Chem. Int. Ed.*, **41**, 48 (2002).
[14] V.R. Thalladi, H.-C. Weiss, D. Blaser, R. Boese, A. Nangia, G.R. Desiraju. *J. Am. Chem. Soc.*, **120**, 8702 (1998).
[15] J.D. Dunitz, R. Taylor. *Chem. Eur. J.*, **3**, 89 (1997).
[16] D. Chopra, T.N.G. Row. *Cryst. Growth Des.*, **6**, 1267 (2006).
[17] F. Leroux. *ChemBioChem.*, **5**, 644 (2004).
[18] A.T. Hulme, S.L. Price, D.A. Tocher. *J. Am. Chem. Soc.*, **127**, 1116 (2005).
[19] J.M. Harrowfield, S. Maghaminia, A.A. Soudi. *Inorg. Chem.*, **43**, 1810 (2004).
[20] J.M. Harrowfield, F. Marandi, A.A. Soudi. *Inorg. Chim. Acta*, **358**, 4099 (2005).
[21] (a) F. Marandi, A. Morsali, A.A. Soudi. *Z. Anorg. Allg. Chem.*, **633**, 661 (2007); (b) F. Marandi, N. Asghari, M. Ghorbanloo, A.A. Soudi, P. Mayer. *Z. Anorg. Allg. Chem.*, **633**, 536 (2007).
[22] (a) F. Marandi, P. McArdle, B. Mirtamizdoust, A.A. Soudi. *J. Coord. Chem.*, **60**, 891 (2007); (b) F. Marandi, N. Asghari, M. Ghorbanloo, P. McArdle. *J. Coord. Chem.*, **61**, 1545 (2008).
[23] J.M. Harrowfield, H. Miyamae, B.W. Skelton, A.A. Soudi, A.H. White. *Aust. J. Chem.*, **49**, 1165 (1996).
[24] A. Altomare, M.C. Burla, M. Camalli, G.L. Cascarano, C. Giacovazzo, A. Guagliardi, A.G.G. Moliterni, G. Polidori, R. Spagna. *J. Appl. Crystallogr.*, **32**, 115 (1999).
[25] G.M. Sheldrick. *SHELXS-97 and SHELXL-97, Programs for the Solution and Refinement of Crystal Structures*, Göttingen, Germany (1997).

[26] G.M. Sheldrick. *SHELXTL Version 5.1*, Bruker AXS Inc., Madison, WI, USA (1998).
[27] L.J. Farrugia. *J. Appl. Crystallogr.*, **30**, 565 (1997).
[28] L. Shimoni-Livny, J.P. Glusker, C.W. Brock. *Inorg. Chem.*, **37**, 1853 (1998).
[29] R.D. Hancock, M.S. Shaikjee, S.M. Dobson, J.C.A. Boeyens. *Inorg. Chim. Acta.*, **154**, 229 (1998).
[30] A.A. Soudi, F. Marandi, A. Ramazani, E. Ahmadi, A. Morsali. *C. R. Chimie*, **8**, 157 (2005).
[31] (a) F. Marandi, B. Mirtamizdoust, S. Chantrapromma, H.-K. Fun. *Anorg. Allg. Chem.*, **633**, 1329 (2007);
     (b) A. Morsali, A.R. Mahjoub. *Solid State Sci.*, **7**, 1429 (2005).
[32] K. Reichenbacher, H.I. Suss, J. Hulliger. *Chem. Soc. Rev.*, **34**, 22 (2005).
[33] D.L. Reger, R.F. Semeniuc, V. Rassolov, M.D. Smith. *Inorg. Chem.*, **43**, 537 (2004).
[34] R.S. Rowland, R. Taylor. *J. Phys. Chem.*, **100**, 738 (1996).
[35] C. Janiak. *J. Chem. Soc., Dalton Trans.*, 3885 (2000).
[36] (a) T. Dorn, C. Janiak, K. Abu-Shandi. *CrystEngComm*, **7**, 633 (2005); (b) K. Abu-Shandi, H. Winkler,
     H. Paulsen, R. Glaum, B. Wu, C. Janiak. *Z. Anorg. Allg. Chem.*, **631**, 2705 (2005); (c) S. Banerjee,
     A. Ghosh, B. Wu, P.-G. Lassahn, C. Janiak. *Polyhedron*, **24**, 593 (2005); (d) S. Banerjee, B. Wu,
     P.-G. Lassahn, C. Janiak, A. Ghosh. *Inorg. Chim. Acta*, **358**, 535 (2005).